

Electrokinetic Control of Viscous Fingering

Mohammad Mirzadeh¹ and Martin Z. Bazant^{1,2,*}

¹*Department of Chemical Engineering, Massachusetts Institute of Technology, MA 02139.*

²*Department of Mathematics, Massachusetts Institute of Technology, MA 02139.*

(Dated: March 20, 2022)

We present a theory of the interfacial stability of two immiscible electrolytes under the coupled action of pressure gradients and electric fields in a Hele-Shaw cell or porous medium. Mathematically, our theory describes a phenomenon of “Vector Laplacian Growth”, in which the interface moves in response to the gradient of a vector-valued potential function through a generalized mobility tensor. Physically, we extend classical Saffman-Taylor problem to electrolytes by incorporating electrokinetic phenomena. A surprising prediction is that viscous fingering can be controlled by varying the injection ratio of electric current to flow rate. Beyond a critical injection ratio, stability depends only upon the relative direction of flow and current, regardless of the viscosity ratio. Possible applications include porous materials processing, electrically enhanced oil recovery, and electrokinetic remediation of contaminated soils.

Interfacial instability is the precursor to pattern formation in a variety of physical and chemical processes [1, 2]. This fascinating topic covers a broad range of phenomena such as dendritic growth due to the Mullins-Sekerka instability in solidification [3, 4], fractal growth due to diffusion-limited aggregation [5] or metal electrodeposition [6] in fluid flows [7], crease formation and wrinkling of combustion fronts due to the Darrieus-Landau instability [8, 9], and viscous fingering in Hele-Shaw cells [10] and porous media [11] due to the Saffman-Taylor instability [12, 13].

Interfacial instabilities are usually undesirable, but difficult to control. In secondary oil recovery, viscous fingering of injected liquids leads to nonuniform displacement and residual trapping of oil [11, 14], and dendritic growth is a major safety concern for metal anodes in rechargeable batteries [15]. There are signs, however, that instability may be avoided if the interface is driven by multiple opposing forces. For instance, it was recently observed that dendritic growth can be suppressed in charged porous media [16] if preceded by deionization shock wave [17], whose stable propagation in cross flow also enables water purification by shock electro dialysis [18, 19].

Here, we consider the interfacial stability of two immiscible electrolytes in a Hele-Shaw cell where the interface is set into motion by both the pressure-driven and electro-osmotic flows. Remarkably, we find that electrokinetic coupling influence interfacial stability and, under certain conditions, can eliminate viscous fingering. This phenomenon illustrates the rich physics of “Vector Laplacian Growth” (VLG), a general mathematical model of interfacial dynamics driven by the gradient of a vector-valued potential function through a generalized mobility tensor. The “one-sided” VLG model (with field gradients only on one side of the interface) is known to be unstable, leading to fractal patterns, during growth [7] and stable, resulting in smooth collapse, during retreat [20, 21]. Our theory shows that stable growth is also possible, if field gradients exist on both sides of the interface.

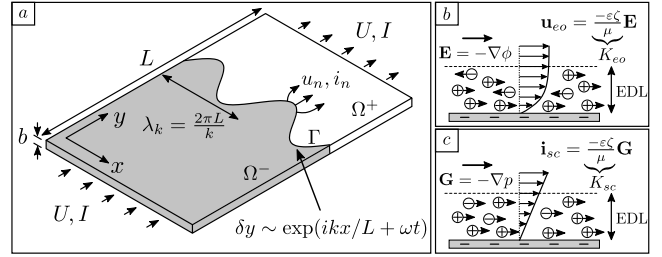


FIG. 1. Schematic of flow in a rectangular Hele-Shaw cell. (a) The interface (Γ) between two immiscible electrolytes moves under the coupled action of pressure gradient and electric field as described by the electrokinetic response of the cell. (b) In addition to the pressure-driven flow, the electric field exerts a net force on ions in the Electric Double Layer (EDL), resulting in the electro-osmotic flow. (c) Similarly, in addition to the Ohmic current driven by the electric field, the pressure-driven flow advects charges in the EDL, resulting in the streaming current.

In the classical viscous fingering problem, the fluid flow in a Hele-Shaw cell can be approximated as quasi two-dimensional if the cell gap, b , is much smaller than the lateral dimension, L (see fig 1). In this case, the gap-averaged velocity of each fluid is given by:

$$\mathbf{u}^{\pm} = -\frac{b^2}{12\mu^{\pm}}\nabla p^{\pm}, \quad \nabla \cdot \mathbf{u}^{\pm} = 0 \quad (1)$$

where ‘-’ and ‘+’ superscripts denote invading and receding fluids, μ and p are viscosity and pressure of each fluid, and ∇ is the in-plane gradient operator. At the interface, the pressure jump is given by the Young-Laplace equation, while the normal velocity is continuous:

$$[[p]] = \gamma\kappa, \quad [[\hat{\mathbf{n}} \cdot \mathbf{u}]] = 0, \quad (2)$$

where $[[a]] \equiv a^+ - a^-$ denotes the jump of variable ‘ a ’ across the interface, γ is the surface tension, and κ is the in-plane curvature. More generally, these conditions

must be modified to take the finite lubrication film thickness into account if the receding fluid is perfectly wetting [11, 22]. The interface moves with the local fluid velocity,

$$\frac{d\mathbf{x}}{dt} = (\hat{\mathbf{n}} \cdot \mathbf{u})\hat{\mathbf{n}}, \quad (3)$$

and the far-field flow is uniform.

Linear stability analysis of Eqs. (1)–(3), initiated by Chuoke *et al.* [13] and Saffman and Taylor [12], reveals that stable displacement is only possible if the advancing fluid is more viscous:

$$\text{Stable: } M = \frac{\mu^-}{\mu^+} > 1. \quad (4)$$

In the opposite case, $M < 1$, the interface is unstable to perturbations of sufficiently long wavelength, and the less viscous fluid forms “fingers” of lower resistance through the more viscous fluid. Specifically, the growth rate, ω , of a normal mode $\delta y \sim \exp(ikx/L + \omega t)$ satisfies the dispersion relation [10, 11]:

$$\omega = \frac{k}{L} \left(U \frac{\mu^+ - \mu^-}{\mu^+ + \mu^-} - \frac{\gamma b^2 k^2}{12L^2(\mu^+ + \mu^-)} \right), \quad (5)$$

where k is the wavenumber. Perturbation wavelengths longer than $\lambda_{cr} = \pi b \sqrt{\gamma/3U(\mu^+ - \mu^-)}$ are unstable, and the maximum growth rate arises for $\lambda_m = \sqrt{3}\lambda_{cr}$.

Most materials naturally acquire charge in aqueous solutions from the dissociation of surface groups, such as silanol [23], for glass in Hele-Shaw cells or silicate minerals in underground reservoirs. The screening of surface charge by mobile ions leads to the formation of electric double layers (EDL) and associated electrokinetic phenomena [24]. An electric field parallel to the charged surface acts on EDL charge to drive “electro-osmotic” flow \mathbf{u}_{eo} , while pressure-driven flow drives “streaming current” \mathbf{i}_{sc} due to the advection of EDL charge (Fig. 1). For typical situations of fixed surface charge, the electrokinetic response is linear in the driving forces, i.e. $\mathbf{u}_{eo} = -K_{eo}\nabla\phi$ and $\mathbf{i}_{sc} = -K_{sc}\nabla p$, where ϕ is the electrostatic potential. The electro-osmotic mobility, K_{eo} , and the streaming conductance, K_{sc} , satisfy Onsager’s reciprocal relation [25, 26], $K_{eo} = K_{sc}$, and for thin EDL (gaps, $b \sim 0.1 - 1$ mm, much larger the EDL thickness, $\lambda_D \sim 1 - 10$ nm), are given by the Helmholtz-Smoluchowski relation [24], $K_{eo} = -\varepsilon\zeta/\mu$, where ε is the electrolyte permittivity.

When linear electrokinetic phenomena are considered, a VLG model can thus be written in terms of a tensorial flux, $\mathbf{F} = (\mathbf{u}, \mathbf{i})^T$, proportional to the gradient of a vector-valued potential, $\Phi = (p, \phi)^T$:

$$\mathbf{F}^\pm = -\mathbb{K}^\pm \nabla \Phi^\pm, \quad \nabla \cdot \mathbf{F}^\pm = \mathbf{0}, \quad (6)$$

where \mathbb{K} is the electrokinetic mobility tensor:

$$\mathbb{K} = \begin{pmatrix} K_h & K_{eo} \\ K_{eo} & K_e \end{pmatrix}. \quad (7)$$

$K_h = b^2/12\mu$ is the hydraulic Darcy conductivity, and $K_e = \sigma$ is the electrical Ohmic conductivity of the cell. The Second Law of Thermodynamics requires positive definite \mathbb{K} to ensure positive dissipation rate [27, 28], i.e.:

$$-\nabla \Phi \cdot \mathbf{F} = \nabla \Phi^T \mathbb{K} \nabla \Phi > 0. \quad (8)$$

At the interface, the pressure and total velocity satisfy the jump conditions given by Eq. (2), while the potential and normal component of the total current are continuous, which can be compactly expressed as:

$$[\Phi] = (\gamma\kappa, 0)^T, \quad [\hat{\mathbf{n}} \cdot \mathbf{F}] = \mathbf{0}. \quad (9)$$

Far from the interface in a planar geometry, the fluxes are assumed to be uniform, $\lim_{y \rightarrow \pm\infty} \mathbf{F}_y = \mathbf{F}_\infty = (U, I)^T$. Equations (6) and (9), along with the kinematic condition (3), determine the interface motion.

As for classical problem, we consider the linear stability of a planar interface subjected to a sinusoidal perturbation, $\delta y \sim \exp(ikx/L + \omega t)$, and seek solutions of the form $\Phi^\pm = \Phi_0^\pm + \epsilon \Phi_1^\pm$ in the limit of $\epsilon \ll 1$. From Eq. (6), the base state is linear, i.e. $\Phi_0^\pm = -\mathbb{K}^{\pm-1} \mathbf{F}_\infty (y - Ut)$, while $\Phi_1^\pm = \mathbf{A}_1^\pm \exp(ikx/L + \omega t) \exp(\mp k(y - Ut)/L)$, where \mathbf{A}_1^\pm are evaluated using the jump condition (9). Applying the kinematic condition (3) then yields the growth rate:

$$\omega = \frac{k}{L} \left(F - \gamma G \frac{k^2}{L^2} \right), \quad (10)$$

where F and G are given by

$$F = U \frac{[\mathbb{K}_{eo}]\{K_{eo}\} - [\mathbb{K}_h]\{K_e\}}{\det\{\mathbb{K}\}} + 2I \frac{K_h^+ K_{eo}^- - K_h^- K_{eo}^+}{\det\{\mathbb{K}\}},$$

$$G = \frac{K_h^+ \det \mathbb{K}^- + K_h^- \det \mathbb{K}^+}{\det\{\mathbb{K}\}}, \quad (11)$$

and $\{a\} \equiv a^+ + a^-$. Note that the classical dispersion relation (5) is recovered in the absence of electrokinetic phenomena, $K_{eo}^\pm = 0$. From the Second Law (8), it follows that $G > 0$, ensuring that surface tension effects are stabilizing. Therefore, $F < 0$ is a *sufficient* condition for stability. For $F > 0$, a perturbation of wavelength longer than $\lambda_{cr} = 2\pi\sqrt{\gamma G/F}$ is unstable, and $\lambda_m = \sqrt{3}\lambda_{cr}$ is the most unstable wavelength.

To simplify equation (11), we note that the electrokinetic coupling coefficient [29], $\alpha = K_{eo}^2/K_h K_e$, is typically small, while $0 \leq \alpha < 1$ from Eq. (8). For $\alpha \ll 1$, the critical wavelength may be approximated as:

$$\lambda_{cr} = \pi b \sqrt{\frac{\gamma}{3U[\mu] + 6I[\varepsilon\zeta]/\{\sigma\}}}. \quad (12)$$

While the classical instability is controlled by the viscosity ratio (Eq. (4)), our theory predicts that the injection ratio, I/U , can be tuned *independently* to control interfacial stability (Fig. 2a):

$$\text{Stable: } \frac{M-1}{M+1} > A \frac{SZ-1}{SZ+1}, \quad (13)$$

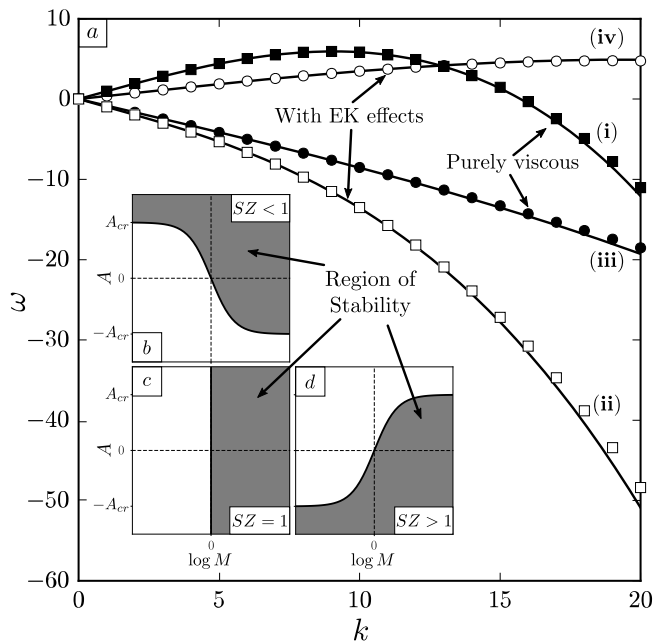


FIG. 2. Linear stability analysis of a planar interface. (a) The non-dimensional growth rate ω (scaled with U/L) versus the wave number k . Solid lines represent the theory (see eq. (10)) while symbols are numerically computed growth rates, obtained by evolving a small-amplitude initial perturbation ($\epsilon = 10^{-3}$) for each wavenumber. Shown are classical results (no EK effects) for (i) unfavorable ($M = 0.01$) and (iii) favorable ($M = 10$) viscosity ratios. When electrokinetic effects are present, stability can be manipulated by adjusting the injection ratio, resulting in either (ii) suppression of viscous fingering ($M = 0.01, SZ = R = 100, A \approx -1.98$), or (iv) electrokinetic fingering ($M = SZ = R = 10, A \approx 1.45$). Here, $R = \sigma^-/\sigma^+$ is the conductivity ratio and the remaining parameters are defined via equation (14). In all cases, the effective Capillary number, $Ca = 12L^2U\mu^+/\gamma b^2$, is set to 250. (b–d) The shaded area illustrates the region of stability as approximated by equation (13). Interestingly, this region is symmetrical around $SZ = 1$, for which classical results are recovered.

in terms of the following dimensionless ratios:

$$S = \frac{\varepsilon^-}{\varepsilon^+}, \quad Z = \frac{\zeta^-}{\zeta^+}, \quad M = \frac{\mu^-}{\mu^+}, \quad A = \frac{I(-\varepsilon\bar{\zeta})}{U\bar{\mu}\bar{\sigma}}, \quad (14)$$

where the over-bar indicates average values, e.g. $\bar{\varepsilon\zeta} = (\varepsilon^+\zeta^+ + \varepsilon^-\zeta^-)/2$. Electrokinetic effects require $SZ \neq 1$, and stability is possible if the injection ratio is larger than $|(M-1)(SZ+1)/(SZ-1)(M+1)|$, and has the “correct” sign, depending on the magnitude of SZ (see Fig. 2). Above a critical injection ratio, $A_{cr} = |(SZ+1)/(SZ-1)|$, stability is entirely determined by the sign of injection ratio and is, remarkably, independent of the viscosity ratio. Physically, negative injection ratios denote opposite direction of current and flow. These observations are illustrated in figure 2b–d.

Motivated by secondary oil recovery, it is interesting

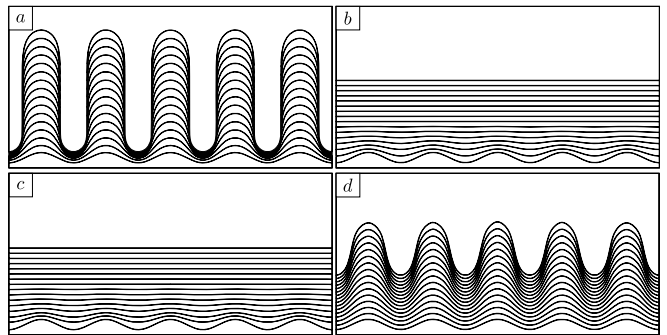


FIG. 3. Numerical simulation of the interfacial dynamics for an initial perturbation. The interface moves upward and its location is drawn at equal time intervals. (a) Viscous fingering for an unfavorable viscosity ratio $M = 0.01$ and (b) its suppression using negative injection ratio (same parameters as in fig. 2a-ii). (c) Stable displacement for favorable viscosity ratio $M = 10$ and (d) formation of electrokinetic fingering with positive injection ratio (same parameters as in fig. 2a-iv).

to consider the limit when $M \ll 1$, $SZ \gg 1$, and $R = \sigma^-/\sigma^+ \gg 1$, e.g. when water is pushing oil toward extraction wells. In this case, negative current injection shifts the critical wavelength to longer values and reduces viscous fingering. Stable displacement is possible if $I > I_{cr}$, where:

$$I_{cr} \approx \frac{U}{2} \frac{\mu^o}{\mu^w} \frac{\sigma^w}{K_{eo}^w}. \quad (15)$$

For $U = 1$ mm/min in a 1 mM KCl solution with $\zeta = -50$ mV and $\mu^w/\mu^o = 0.1$, the critical current is fairly small, $I_{cr} \sim 4$ mA/cm², but a large critical electric field is required to drive this current across the poorly conducting oil region:

$$E_{cr} \approx \frac{U}{4} \frac{\mu^o}{\mu^w} \frac{\sigma^w}{\sigma^o} \frac{1}{K_{eo}^w}. \quad (16)$$

Even for a modest value of $\sigma^w/\sigma^o = 10$, complete suppression of viscous fingering requires $E_{cr} \sim 150$ V/cm. The required voltage could be lowered by reducing the conductivity ratio or electrode separations. Nonetheless, partial stabilization (with enhanced oil recovery) is still viable with electric fields below the critical value.

To further support our theory, we numerically solve the VLG model using the Voronoi Interface Method [30] to discretize the conservation equations (6) subjected to the interface jump conditions (9) while utilizing the level-set framework [31] to represent the moving interface. Furthermore, we use dynamically adaptive quadtree grids [32] as well as parallel algorithms [33] for fast and high-fidelity simulations. Figure 3 illustrates the interfacial dynamics of an initial perturbation for unfavorable, 3-(a,b), and favorable, 3-(c,d), viscosity ratios. As predicted, interfacial stability can be manipulated by adjusting the injection ratio.

It is straight-forward to extend the analysis for the radial Hele-Shaw cell geometry [11, 34] where an invading fluid is injected at a point to push the second fluid outward. If the interface is initially assumed to be circular, the growth rate of an azimuthal perturbation of the form $\delta r \sim \exp(ik\theta + \omega t)$, is given via:

$$\omega = -\frac{U}{r} + \frac{k}{r} \left(F - \gamma G \frac{(k^2 - 1)}{r^2} \right), \quad (17)$$

where r is the initial radius and F and G are still given by equation (11). Once again, $F < 0$ is a sufficient condition for stability. Therefore, the stability estimate in equation (13) could be used in radial geometry if velocity, U , and current density, I , are replaced by the total flow rate, Q_0 , and total current, I_0 , respectively. Figure 4 illustrates numerical simulation of interface evolution in a radial Hele-Shaw cell geometry for an unstable viscosity ratio of $M = 0.01$. The instability is entirely suppressed when current is injected the opposite direction.

The possibility of manipulating interfacial instabilities is quite exciting. The idea of controlling viscous fingering using cell geometry has been recently discussed [35], but in general situations, it is still possible to control injection ratios, e.g. by controlling electrode placement and the applied potential. Hele-Shaw cell experiments could be used to check these predictions and test the validity of our assumptions. In particular, electrokinetic phenomena depend on which liquid is contact with the surface. Here, we have neglected the possibility of lubrication films and gravity currents [36], which would require more complicated depth-averaging and electrokinetics at the liquid-liquid interface [37], perhaps amenable to conformal-map dynamics [7, 38]. We have also ignored non-linear electrohydrodynamic effects [39] which might cause interfacial instabilities at higher electric fields [40–42].

Although our theory is for immiscible electrolytes, it may also describe diffuse interfaces involving strong ion concentration gradients, e.g. deionization shocks in charged porous media [17] or pH fronts in electrokinetic remediation of contaminated soil [43]. Since the ζ -potential is a strong function of pH and salt concentration [23], it is expected to be non-uniform in these systems. Therefore our results might be relevant to the stability of ion concentration fronts [17], although a more detailed analysis including surface charge regulation may be required.

Finally, we caution that viscous fingering is more complicated in porous media than in Hele-Shaw cells, due to permeability variations, capillary effects, and surface wettability [44, 45]. Since electrokinetic couplings derive from surfaces, we expect strong dependence on surface wettability whereas permeability variations might have limited impact due to disproportionate scaling of hydraulic and electro-osmotic mobilities with the pore size, possibly resulting in a more uniform displacement. Nonetheless, further investigation is required to quantify

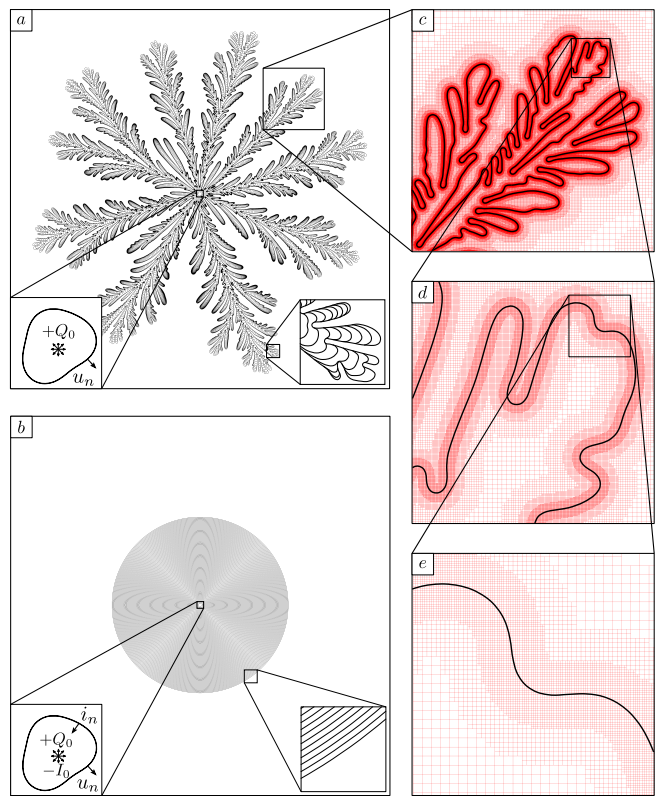


FIG. 4. Numerical simulation of the interfacial dynamics in a radial Hele-Shaw cell. (a) An initial “bubble” (left inset) separates two immiscible ($M = 0.01$) and grows outward due to a positive flow source in the middle. The interface location, drawn at equal time intervals (right inset), reveals a complex pattern due to successive growth and tip-splitting. (b) The viscous fingering is entirely suppressed by injecting electric current in the opposite direction, resulting in a uniform circular growth (same parameters as in fig. 2a-ii). (c-e) Snapshot of the final pattern in (a), illustrating the level of details that is captured in the simulation.

the degree to which electrokinetic phenomena can control interfacial stability in porous media.

This work was supported by a seed grant from the MIT Energy Initiative. The first author acknowledges fruitful discussions with Amir A. Pahlavan during the course of the project. The authors acknowledge the Texas Advanced Computing Center (TACC) at The University of Texas at Austin for providing HPC and visualization resources that have contributed to the research results reported within this paper. This work used the Extreme Science and Engineering Discovery Environment (XSEDE), which is supported by National Science Foundation grant number ACI-1548562.

* bazant@mit.edu

[1] D. A. Kessler, J. Koplik, and H. Levine, *Advances in*

- Physics **37**, 255 (1988).
- [2] P. Pelcé and A. Libchaber, *Dynamics of curved fronts* (Elsevier, 2012).
- [3] W. W. Mullins and R. F. Sekerka, Journal of applied physics **34**, 323 (1963); Journal of Applied Physics **35**, 444 (1964).
- [4] J. Langer, Reviews of Modern Physics **52**, 1 (1980).
- [5] T. A. Witten and L. M. Sander, Physical Review B **27**, 5686 (1983).
- [6] R. Brady and R. Ball, Nature **309**, 225 (1984).
- [7] M. Z. Bazant, J. Choi, and B. Davidovitch, Physical Review Letters **91**, 045503 (2003).
- [8] G. Darrieus, Unpublished works presented at “La Technique Moderne” (1938) and “Congrès de Mécanique Appliquée” (1945). L. Landau, Acta physicochim. URSS **19**, 77 (1944).
- [9] G. I. Sivashinsky, Annual Review of Fluid Mechanics **15**, 179 (1983); M. Matalon, Annu. Rev. Fluid Mech. **39**, 163 (2007).
- [10] D. Bensimon, L. P. Kadanoff, S. Liang, B. I. Shraiman, and C. Tang, Reviews of Modern Physics **58**, 977 (1986).
- [11] G. M. Homsy, Annual review of fluid mechanics **19**, 271 (1987).
- [12] P. G. Saffman and G. Taylor, in *Proceedings of the Royal Society of London A: Mathematical, Physical and Engineering Sciences*, Vol. 245 (The Royal Society, 1958) pp. 312–329.
- [13] R. Chuoke, P. Van Meurs, and C. van der Poel, Pet. Trans. AIME **216** (1959).
- [14] S. B. Gorell and G. Homsy, SIAM Journal on Applied Mathematics **43**, 79 (1983).
- [15] W. Xu, J. Wang, F. Ding, X. Chen, E. Nasybulin, Y. Zhang, and J.-G. Zhang, Energy & Environmental Science **7**, 513 (2014).
- [16] J.-H. Han, M. Wang, P. Bai, F. R. Brushett, and M. Z. Bazant, Scientific Reports **6** (2016).
- [17] A. Mani and M. Z. Bazant, Physical Review E **84**, 061504 (2011).
- [18] D. Deng, E. V. Dydek, J.-H. Han, S. Schlumpberger, A. Mani, B. Zaltzman, and M. Z. Bazant, Langmuir **29**, 16167 (2013).
- [19] S. Schlumpberger, N. B. Lu, M. E. Suss, and M. Z. Bazant, Environmental Science & Technology Letters **2**, 367 (2015).
- [20] M. Z. Bazant, Physical Review E **73**, 060601 (2006).
- [21] C. H. Rycroft and M. Z. Bazant, Proceedings of the Royal Society A: Mathematical, Physical and Engineering Science **472**, 20150531 (2016).
- [22] C.-W. Park and G. Homsy, Journal of Fluid Mechanics **139**, 291 (1984).
- [23] B. J. Kirby and E. F. Hasselbrink, Electrophoresis **25**, 187 (2004).
- [24] W. B. Russel, D. A. Saville, and W. R. Schowalter, *Colloidal dispersions* (Cambridge university press, 1989); J. Lyklema, *Fundamentals of interface and colloid science: Solid-Liquid Interfaces*, Vol. 2 (Academic press, 1995).
- [25] L. Onsager, Physical review **37**, 405 (1931).
- [26] M. Z. Bazant, Physical Review Fluids **1**, 024001 (2016).
- [27] S. R. De Groot and P. Mazur, *Non-equilibrium thermodynamics* (Courier Corporation, 2013).
- [28] P. B. Peters, R. Van Roij, M. Z. Bazant, and P. M. Biesheuvel, Physical Review E - Statistical, Nonlinear, and Soft Matter Physics **93**, 1 (2016).
- [29] F. H. J. Van Der Heyden, D. J. Bonthuis, D. Stein, C. Meyer, and C. Dekker, Nano Letters **6**, 2232 (2006); Nano Letters **7**, 1022 (2007).
- [30] A. Guittet, M. Lepilliez, S. Tanguy, and F. Gibou, Journal of Computational Physics **298**, 747 (2015).
- [31] S. Osher and J. Sethian, Journal of computational physics **79**, 12 (1988); S. Osher and R. Fedkiw, *Level set methods and dynamic implicit surfaces*, Vol. 153 (Springer Science & Business Media, 2006); J. A. Sethian, *Level set methods and fast marching methods: evolving interfaces in computational geometry, fluid mechanics, computer vision, and materials science*, Vol. 3 (Cambridge university press, 1999).
- [32] C. Min and F. Gibou, J. Comput. Phys. **225**, 300 (2007).
- [33] M. Mirzadeh, A. Guittet, C. Burstedde, and F. Gibou, Journal of Computational Physics **322**, 345 (2016).
- [34] L. Paterson, Journal of Fluid Mechanics **113**, 513 (1981).
- [35] T. T. Al-Housseiny, P. A. Tsai, and H. A. Stone, Nature Physics **8**, 747 (2012); T. T. Al-Housseiny and H. A. Stone, Physics of Fluids **25**, 092102 (2013).
- [36] I. Eames, M. Gilbertson, and M. Landeryou, Journal of Fluid Mechanics **523**, 261 (2005).
- [37] A. J. Pascall and T. M. Squires, Journal of Fluid Mechanics **684**, 163 (2011).
- [38] T. Robinson and I. Eames, Journal of Engineering Mathematics **103**, 77 (2017).
- [39] J. R. Melcher and G. I. Taylor, Annual Review of Fluid Mechanics **1**, 111 (1969); J. R. Melcher, *Continuum Electromechanics* (1981); *Field-coupled surface waves* (MIT, 1963).
- [40] G. I. Taylor and a. D. McEwan, Journal of Fluid Mechanics **22**, 1 (1965).
- [41] H. Lin, B. D. Storey, M. H. Oddy, C.-H. Chen, and J. G. Santiago, Physics of Fluids **16**, 1922 (2004); C.-H. Chen, H. Lin, S. K. Lele, and J. G. Santiago, Journal of Fluid Mechanics **524**, 263 (2005).
- [42] C. L. Druzgalski, M. B. Andersen, and A. Mani, Physics of Fluids **25**, 110804 (2013).
- [43] R. F. Probst and R. E. Hicks, Science **260**, 498 (1993); A. P. Shapiro and R. F. Probst, Environmental Science & Technology **27**, 283 (1993).
- [44] R. Lenormand, E. Touboul, and C. Zarcone, Journal of Fluid Mechanics **189**, 165 (1988).
- [45] B. Zhao, C. W. MacMinn, and R. Juanes, Proceedings of the National Academy of Sciences **113**, 10251 (2016).